

Characterization of a Zinc/Nickel Plating Bath

Paulo Vieira, Bart Van den Bossche and Alan Rose*
Elsyca, Inc.
Newnan, Georgia, USA

Zinc/nickel electrodeposits have been seen as a viable replacement for cadmium, which has highly desirable properties in many engineering applications, but possesses serious health and environmental drawbacks. In this work, we took a systematic approach to characterize the properties of an existing zinc/nickel plating process through analysis of polarization data and corrosion properties. From this data, computer simulations were performed on a complex aircraft landing gear part to determine the distribution of plate thickness, current density and alloy composition over the geometry of the part, all of which can be used to predict corrosion performance.

Keywords: zinc/nickel plating, alloy plating, alloy composition, roughness, computer simulation, corrosion performance, cadmium replacements

Introduction

Cadmium replacement

For decades a suitable replacement for cadmium has been discussed and debate on the best alternative is still ongoing. Due to the toxic nature of most cadmium salts, the growing environmental pressure to reduce cadmium usage has led some countries to ban the use of cadmium and research for alternatives was intensified. Cadmium is used for several applications due to its lubrication/friction properties in combination with corrosion protection. The lubrication ability of cadmium is an important factor in the fastener industry, providing corrosion protection that doesn't disturb the thread profile along with break-away torques that allow for fasteners to be mated several times without damage.¹

An additional difficulty for the replacement of cadmium is the extensive data collected over the years on cadmium's mechanical and corrosion protection properties on which industries all over the world rely to develop new products.

A wide range of possibilities has been suggested, from electroplated and electroless deposits to physical vapor deposited coatings. Among the candidates to replace cadmium are the zinc-nickel alloys, which can outperform cadmium in corrosion tests, exhibiting a resistance in salt spray test (ASTM B-117) of up to 3000 hr.²

Zinc-nickel corrosion

The Zn/Ni corrosion mechanism has been a target of investigation at least since the 1990s and despite the commitment of several authors, some aspects of the Zn/Ni corrosion mechanism are still under debate.

The initial studies aimed to find a correlation between corrosion protection and nickel content, with several studies reporting slightly different nickel content as the best protective layer (Table 1).

Table 1
Examples of suggested nickel weight content for best corrosion protection

Year	Author	% Ni
1990	C.M. Vlad ³	10 -16%
1991	M. Pushpavanam ⁴	18%
1994	A.M. Alfantazi ⁵	14 - 20%
1997	H. Park ⁶	13 -15%
1999	M. Benballa ⁷	13%
2003	M.H. Sohi ⁸	13%

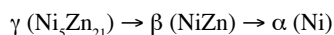
Higher nickel contents lead to additional problems, such as limited ductility (above 20 wt% Ni) or increasing difficulties in passivating the deposits, which is impossible in alloys containing over 25 wt% nickel.⁴

* Corresponding author:
Dr. Alan Rose
Elsyca, Inc.
176 Millard Farmer Ind. Blvd.
Newnan, GA 30263
Phone: (770) 328-1346
E-mail: alan.rose@elsyca.com
Web: www.elsyca.com

Deeper investigations introduced the importance of the phase distribution in the Zn/Ni layer, claiming that corrosion resistance was defined by the type of phase structures present in the deposit, rather than the nickel content alone. Depending on the source, different phase structures have been described for the same nickel content leading to an unclear relationship between phase structure and corrosion resistance (Table 2).

In 1999, Bruet-Hotellaz and co-workers⁹ shed some light on the phase structure debate by concluding that Zn/Ni deposits were not electrodeposited in thermodynamic equilibrium, opening the path to the idea where different process conditions can lead to different phase structures albeit with the same nickel content.

It has also been reported that above 15 wt% nickel, a dezincification process occurs, leading to an alloy more noble than the steel substrate, resulting in the loss of sacrificial properties.¹²



Corrosion of the Zn/Ni layer does not occur uniformly nor at a steady rate. Instead it occurs by a network of cracks with an accelerated corrosion in the first stages, which is then slowed down by its own product of corrosion, $\text{Zn}(\text{OH})_2$.¹² Zinc hydroxide dehydrates in time to form ZnO. However the presence of nickel in the deposit slows down the dehydration process, supporting the idea that $\text{Zn}(\text{OH})_2$ provides a barrier on the affected areas, prolonging the corrosion protection. Zinc oxide has a higher electronic conductivity and for this reason does not slow down the corrosion rate as effectively as its hydroxide.¹¹

This network of cracks visible in the Zn/Ni corroded surface is probably due to internal stress caused by *in situ* hydrogen insertion during the electrodeposition process. This is an important difference with the cadmium corrosion mechanism, which happens slowly and uniformly.¹²

Polarization data

The rotating disc electrode (RDE) is the most popular laboratory electrode due to its simple geometry and electrochemical capabilities. Yet to plate circular coupons, a modified rotating disk electrode (MRDE) was used. It consisted basically of a rotating working electrode in a thermostatically monitored electrolyte (double-walled glass cell with a water cooling / heating circuit), a reference electrode (RE) and a platinum mesh as a counter-electrode (Figs. 1-3).

The working electrode consisted of a steel circular coupon fixed between a steel holder and a plastic cap, resulting in plastic cylinder with a steel disk at the bottom center. The working electrode was placed in the electrochemical cell at a 45° angle to avoid gas blockage of the surface. Linear sweep voltammetry (LSV) was performed using an Autolab PGSTAT30 potentiostat. The reference electrode was connected to the solution by means of a KCl salt bridge, in order to prevent contamination.

Cathodic polarization data was obtained from linear sweep voltammetry (LSV) experiments on the MRDE with a steel working electrode (14 mm diameter), starting from the open circuit potential (OCP) up to a current density significantly higher than the industrially applied current density (approximately 0 to 500 A/m²).

The collected polarization data is still in a raw format and must be corrected for the ohmic potential drop around the MRDE according to Equation 1:

$$\eta = E - RjA \quad (1)$$

where:

η = electrode overpotential vs Ag/AgCl_{sat} reference electrode (V);

E = electrode potential vs Ag/AgCl_{sat} reference electrode (V);

R = ohmic electrolyte resistance around the RDE electrode (Ω);

A = active surface of the disc electrode (m²);

j = cathodic current density on the RDE (A/m²).

The ohmic electrolyte resistance R is obtained in very good approximation from an analytical expression, Equation 2:

$$R = \frac{1}{4\sigma r} \quad (2)$$

where: r = electrode radius (m);

σ = electrolyte conductivity (S/m).

LSV type polarization curves are a common tool to help in understanding an electrochemical process by representing the current density as a function of the applied electrode potential for a given electrolyte. While changing the potential between the working electrode and the reference electrode linearly with time, the current response of the electrolyte is recorded. A typical cathodic polarization curve has three distinct regions, an initial rise of current density up to a plateau followed by a final sharper increase.

Table 2
Examples of reported phase structures as function of nickel content

Source	Wt% Ni											
	5	6	7	8	9	10	11	12	13	14	15	
Thermodynamic Equilibrium ⁹	$\eta + \delta$					δ	$\delta + \gamma$			γ		
Bruet-Hotellaz, <i>et al.</i> ⁹	$\eta_d + \gamma_d$								γ			
Lambert, <i>et al.</i> ¹⁰	$\eta + \gamma$						γ					
Wilcox, <i>et al.</i> ¹¹						γ						
H. Park, <i>et al.</i> ⁶									η	$\eta + \gamma$	γ	



Figure 1—MRDE device with plastic holder (left), coupon (center) and core rod (right).



Figure 2—MRDE laboratory set-up.

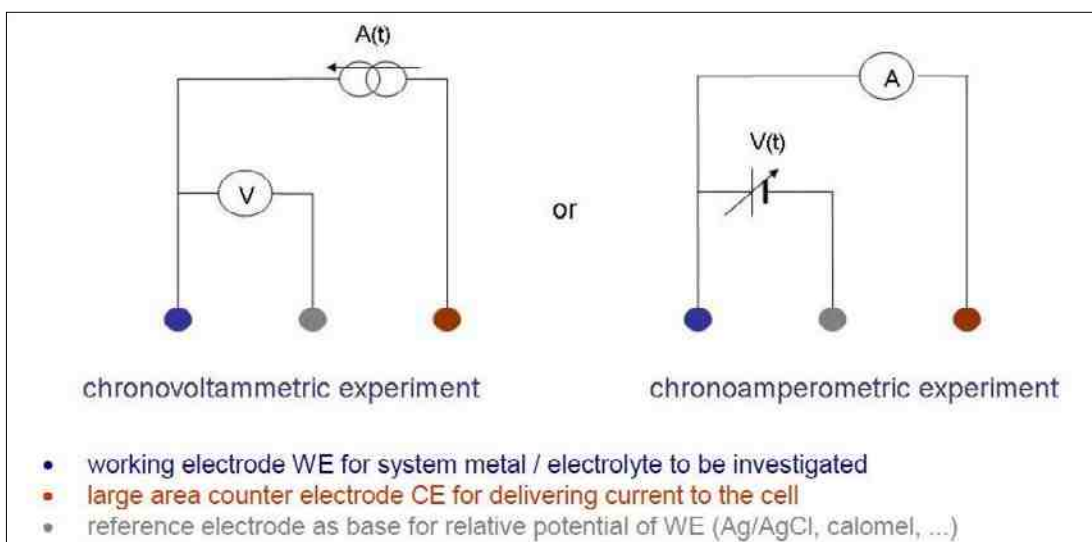


Figure 3—Electric configurations for performing RDE experiments.

The first rise in current density represents the initial stages of the deposition process, where the deposition rate is determined by the overpotential. This is known as the kinetic-controlled region. For higher overpotential values, the kinetic rate of deposition is eventually limited by the speed at which the metal ions are transported to the cathode/electrolyte surface. At this point, the mass transfer limitations will restrict the current to the so-called limiting current value, and a further increase (negative shift) in electrode potential will not have an impact in current density. For even more negative electrode potentials, the mass transfer-controlled region is followed by hydrogen evolution (for aqueous electrolytes), resulting in a sharp increase in current density.

The theoretical expression for the mass transfer limited current density of a rotating disk electrode can be easily computed, using Equation 3:

$$j_{\text{lim},RDE} = -0.62zFD^{2/3}\nu^{-1/6}\omega^{1/2}c \quad (3)$$

where: D = metal ion diffusion coefficient (m^2/sec);
 ω = rotation speed (rad/sec);
 ν = kinematic viscosity (m^2/sec);
 z = metal ion charge (valence);
 F = Faraday's Constant ($96,500 \text{ Coul}/\text{mol}$);
 c = metal ion bulk concentration (M/m^3);
 j = cathodic mass transfer limited current density (A/m^2).

As seen in Fig. 4, Equation 3 indicates that an increase in rotation speed improves the refreshment of ions at the electrode surface, resulting in a shift of the limiting current density to a higher value.

Experimental

The electrolyte characterization presented here is based on a commercially available cyanide-free, alkaline Zn-Ni electrolyte (12 to 15% Ni). To eliminate any start-up problems with a fresh bath, an electrolyte sample from an operating line was requested from a Zn-Ni electroplating company.**

The sample was subjected to a carbonate removal process by lowering the electrolyte temperature below the carbonates' freezing point. This process also drags-out one of the additives, which was replenished back to the operational concentration window prior to this experimental step.

Recommended operational parameters

The operational parameters as recommended by the supplier (excluding additives) are shown in the Table 3.

Table 3
Operational parameters recommended by the electrolyte supplier

Current density (rack)	100 - 300 A/m ²
Current density (barrel)	10 - 150 A/m ²
[Zn], g/L	9.0 - 11.0 g/L
[Ni], g/L	2.0 - 2.8 g/L
Temperature, °C	26°C

** Electrofer IV, Portugal.

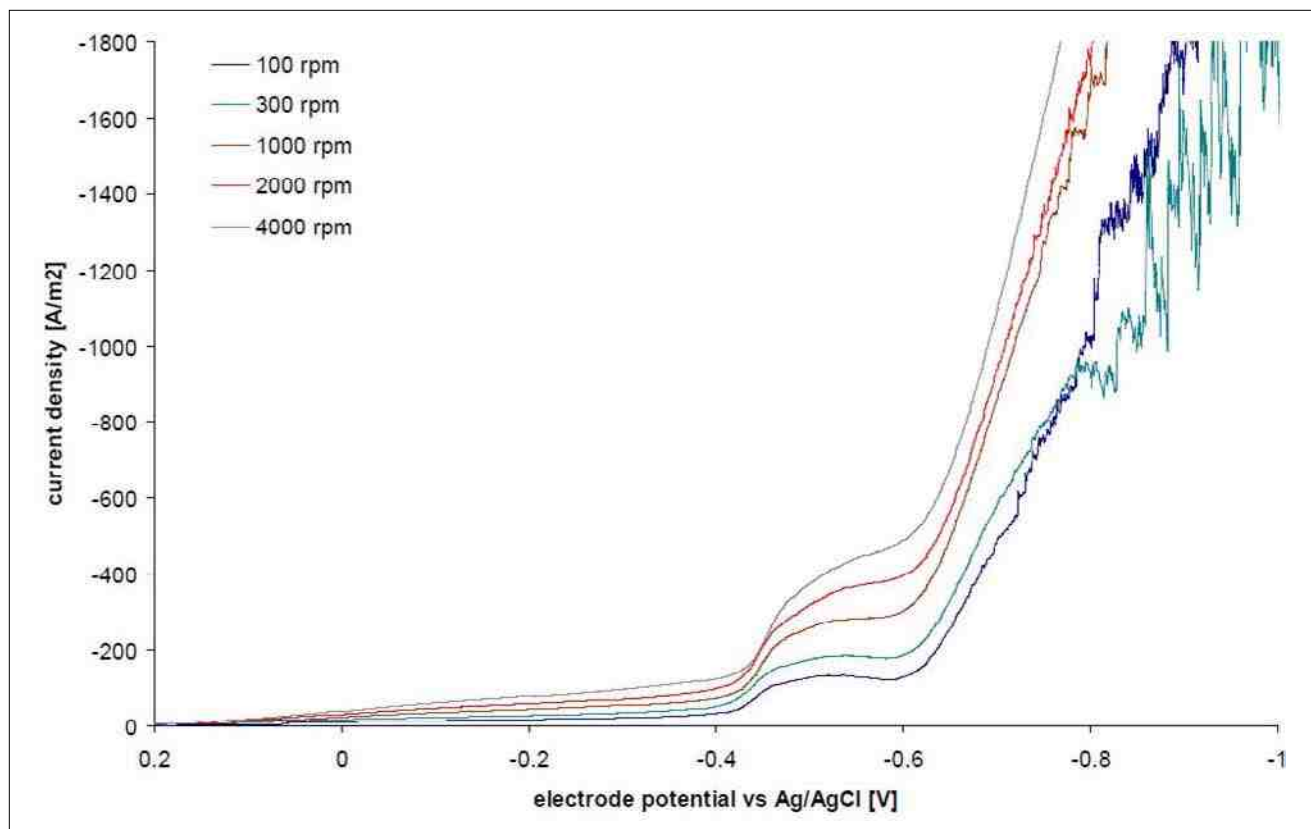


Figure 4—Example of a platinum electrolyte polarization curve.

For the bath sample examined within the scope of this project, the nickel content was at the lower limit of the recommended operational window (*i.e.*, 2.0 g/L).

Cathodic polarization

Cathodic polarization data were recorded as described previously for three different hydrodynamic conditions. Hydrodynamic conditions around rotating electrodes are well known and can be adjusted by setting the rotation speed of the electrode. For the present work, the selected rotation speeds were:

- a) 100 RPM – equivalent to natural convection;
- b) 400 RPM – low forced flow;
- c) 1200 RPM – high forced flow (but still laminar).

Carbon steel coupons were degreased in acetone and then freed from oxides in a chemical pickling solution of hydrochloric acid (10 vol%) for 10 to 15 min.

The conductivity of the electrolyte at 26°C was recorded as 11.5 S/m at a pH value of 13.8.

The polarization curves at these three different rotation speeds are presented in Fig. 5.

The curves each show two plateaus, the first being the nickel deposition limiting current which is consistent with dark nickel-rich areas found at very low current densities. A limiting current plateau is observed, but the increasing slope of this plateau suggests that kinetically-controlled zinc deposition is already taking place. At higher current densities, the zinc deposition limiting cur-

rent occurs, and is followed by a passivation region (preventing a limiting current plateau from occurring). The passivation behavior disappears for even more negative electrode potential values due to the initiation of hydrogen evolution.

At 200 A/m², which is the operational current density that is recommended by the supplier for rack applications, the process is situated in the hydrogen evolution region, implying that both metals are deposited under mass transfer limiting conditions. This enhances the importance of both electrolyte refreshment (flow) and control of the metal concentration in the electrolyte to obtain a relatively constant alloy composition up to very high current densities.

At low current densities, one or both metals might be deposited under kinetic control, and in that case the ratio of plated metals will not be constant.

Below 15 A/m² (with natural convection and moderate forced flow), zinc is not yet in mass transfer limitation and therefore its ratio in the alloy will gradually decrease as current density decreases.

Conductivity has an important impact on the throwing power of the electrolyte. The value as recorded here (11.5 S/m) is at the lower end of industrial aqueous plating baths, hence indicating poor throwing power.

Also, the slope of the polarization curve determines the throwing power of the electrolyte. For this Zn/Ni electrolyte, the entire current density operation window (100 to 300 A/m²) is within a 60 mV potential range. This again indicates a low throwing power of the electrolyte.

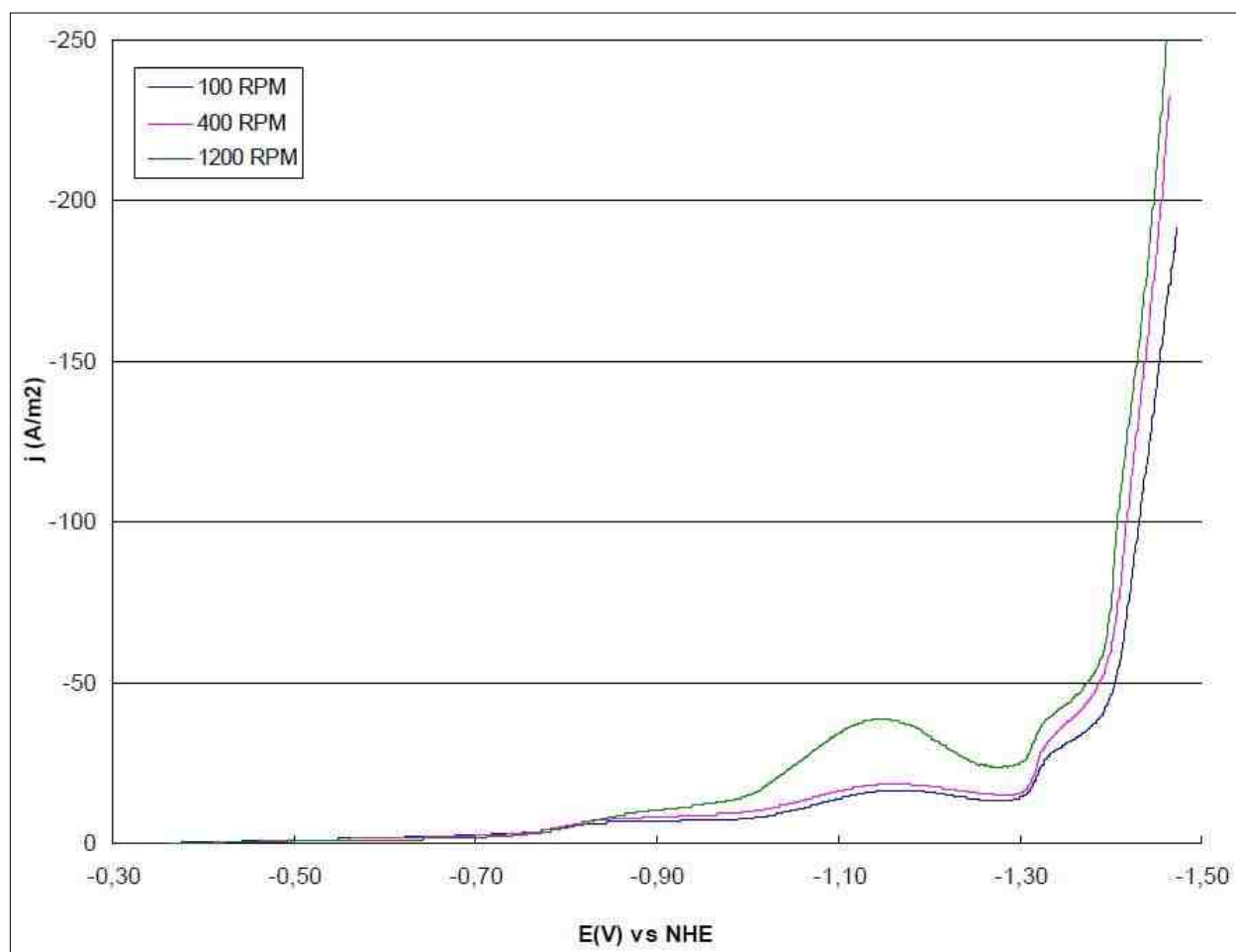


Figure 5—Polarization curves for three different rotation speeds.

Cathodic efficiency

Cathodic efficiency represents the ratio between the current that is used solely in the plating process and the total current applied, including that used in hydrogen gas evolution. The electrolyte supplier claims a cathodic efficiency between 50 and 60%. Since no reference is made to the current density interval involved it is assumed that this efficiency is related to the range of 100 to 300 A/m².

The efficiency noted was indeed obtained within the recommended current density interval [100 to 300 A/m²] although only for higher agitation regimes (Fig. 6). For natural convection and mild forced flow conditions, efficiency values are somewhat smaller and the maximum efficiency is shifted towards lower current densities (100 A/m²).

At very low current densities, the process shows a lower plating efficiency because some of the electrical charge will be lost either to partial reduction of the metals or to reactions with other species present in the electrolyte.

As current density increases, the efficiency sharply rises to its maximum value. Around 50 A/m², hydrogen starts to evolve (Fig. 6), causing a deceleration in plating efficiency increase, and soon hydrogen evolution becomes dominant over the plating process. At this point a maximum efficiency is observed and further increase in current density progressively boosts hydrogen evolution, resulting in a significant efficiency drop.

At higher convection rates, the ion refreshment at the cathode surface is more efficient, causing the limiting current density for both nickel and zinc deposition to be increased. Since the initiation of hydrogen evolution is not affected by hydrodynamics, the peak efficiency value will be shifted to more negative electrode potentials.

Alloy composition

As described earlier, it is generally agreed that above 15 wt% nickel, there is a large drop in corrosion resistance.

The Zn/Ni plating process under study here targets an alloy composition with a nickel content between 12 and 15 wt%. Although much of our data falls within this range, non-conformities can still

be found within the operational window, as seen in Fig. 7. In fact from 100 to 300 A/m², most current densities result in nickel-poor alloys, especially in the case of higher solution convection (Fig. 6).

It has to be remembered that the electrolyte was operated with a nickel concentration at the lower end of the range recommended by the supplier. This is the main cause for the nickel content being below 12 wt% for low current density values. It is reasonable to assume that if the nickel concentration in the electrolyte were increased, a slight increase in nickel content in the deposit would be evident, bringing the low current density deposits above 12 wt% nickel. On the other hand, this correction would also cause the high current density deposits to contain more nickel. At the recommended nickel concentration in the electrolyte (2.0 - 2.8 g/L), the 15 wt% nickel threshold is reached only for very high current densities, but for natural convection, a single 1 wt% increase in nickel content would exceed the 15 wt% nickel limit, even within the operational current density window (100 - 300 A/m²).

It is observed that in the operational current density interval, the alloy composition is only slightly affected by the flow conditions. For higher current densities however, convection becomes increasingly important, and higher convection rates will be required to keep the nickel content in the deposit below 15 wt%.

At very low current densities (< 20 A/m²), another increase in nickel content is observed, but this is easily explained by the fact that the zinc deposition reaction is not yet under mass transfer limitations.

Roughness

Although determination of the deposit nickel content is the main goal of this study, roughness (R_a value) was also evaluated, since roughness could have an impact on the corrosion protection of the layer, especially if the roughness is of the same order of magnitude at the total deposit thickness.

In order to restrict the plating times (mainly for the low current density samples) 2- μ m thick layers were plated. For this reason, a strong influence of the substrate roughness is still observed in the measured deposit roughness values. However, it can be clearly

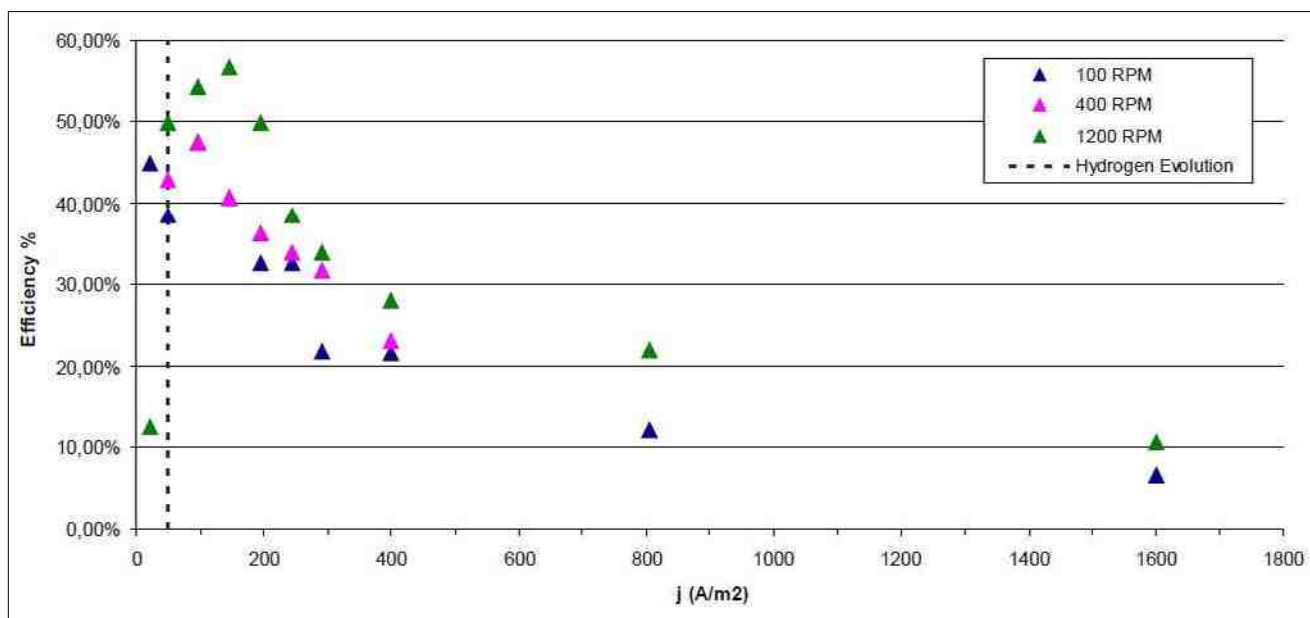


Figure 6—Efficiency as a function of current density for three different rotation speeds.

observed from Fig. 8 that a combination of poor hydrodynamics with high current densities leads to a rapid increase of the observed roughness value. From this set of measurements it can only be concluded that up to a thickness of 2 μm , the Zn-Ni layer follows the roughness of the steel substrate being used.

Taking in to account the achieved thickness of the plated layer, results suggest that the roughness of the layer decreases with increasing layer thickness (Fig. 9). However further tests with a thicker plated layer are required to reach decisive conclusions.

Simulations

Figures 10 to 12 show some preliminary results for the Zn-Ni layer thickness distribution, current density distribution and nickel content distribution, respectively, over a landing gear part of considerable size and geometrical complexity. This simulation was performed using only main anodes at a respectable distance from the part, for an average imposed current density of 300 A/m^2 over the surfaces to be plated. Plating time was set at 30 minutes. The deposit thickness and current density show a huge variation over the part, whereas the nickel content drops below 0.12 wt% in the low current density areas.

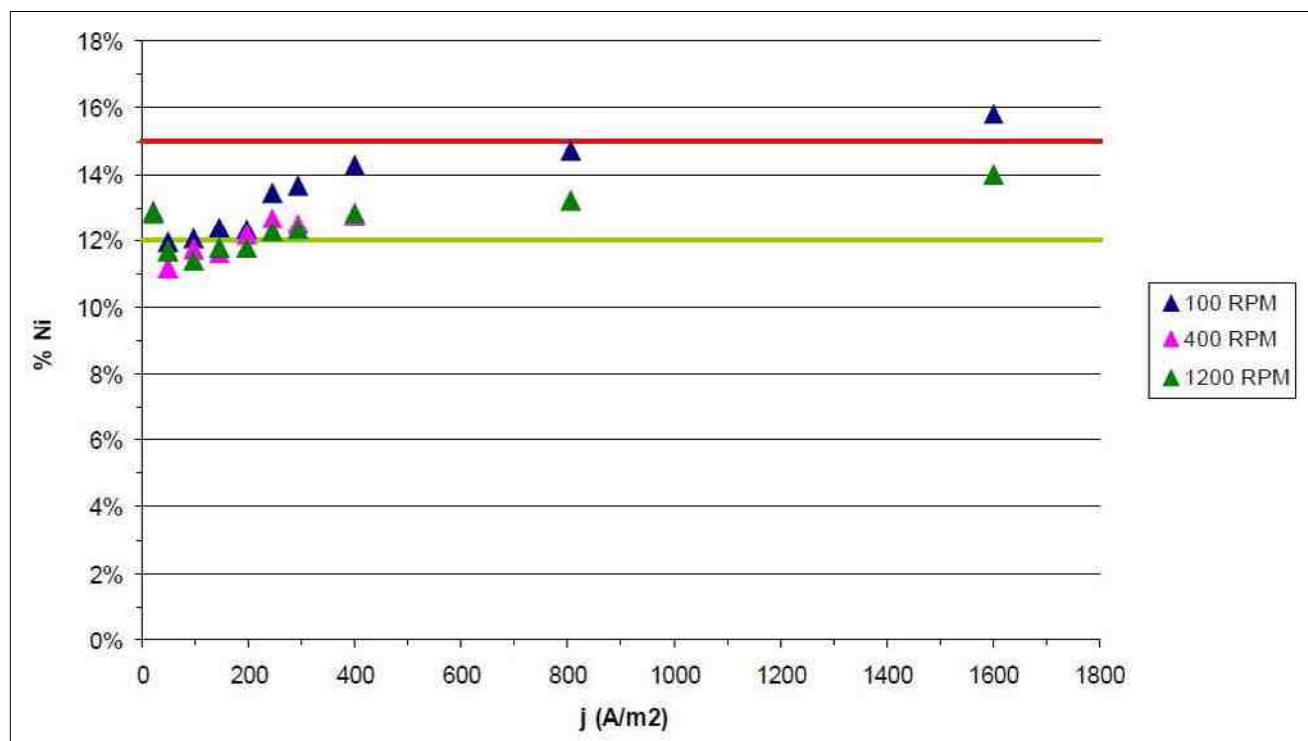


Figure 7—Nickel content in alloy composition.

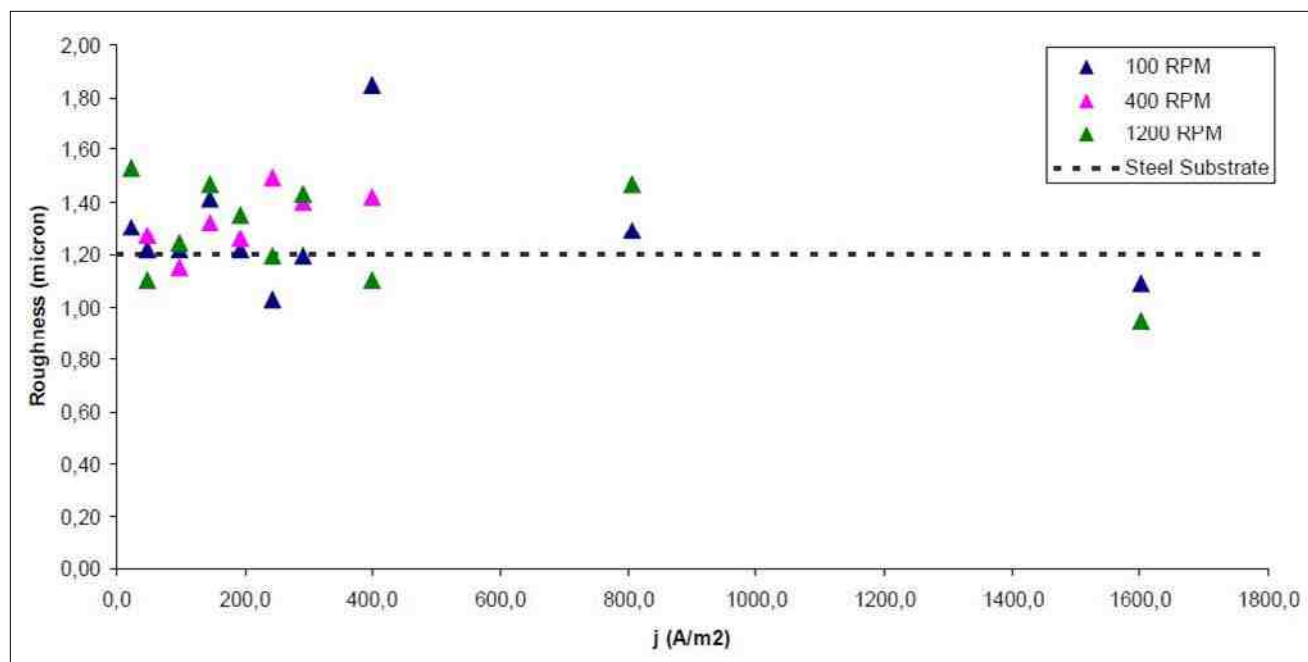


Figure 8—Roughness as a function of current density.

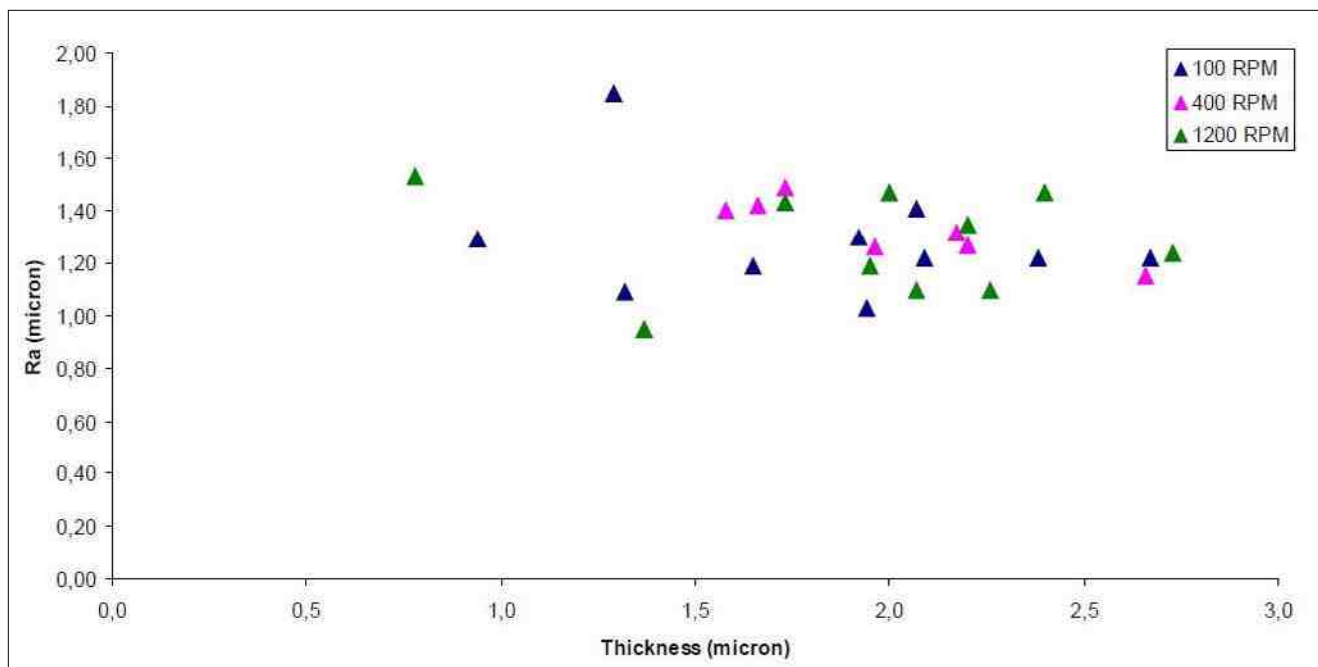


Figure 9—Roughness as a function of layer thickness.

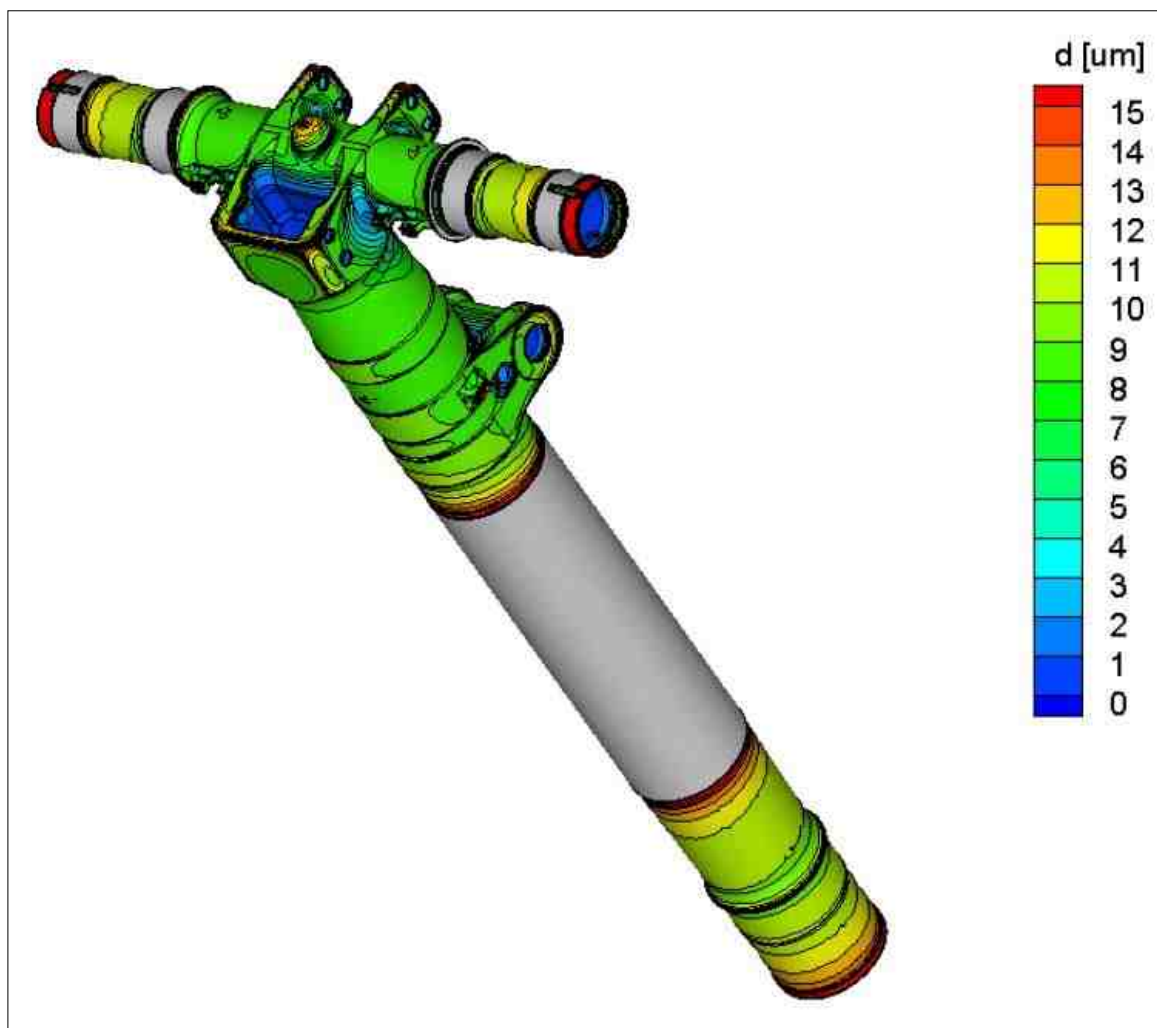


Figure 10—Simulated Zn-Ni layer thickness distribution over a landing gear part.

Discussion

Current density distribution

From a general point of view, the Wagner number is a measure for predicting the degree of non-uniformity in current density distribution over a surface to be plated. Hence also for this Zn-Ni electroplating process, the Wagner number will allow one to predict - to some extent - the degree of non-uniformity that can be expected. The Wagner number is defined in Equation 4:

$$Wa = \frac{\partial(V_c - U_c)/\partial j_c}{\rho L} \quad (4)$$

The numerator represents the “polarization resistance,” or more precisely, the inverse of the slope of the polarization curve at the “working point” (*i.e.*, for the average cathodic current density, j_c). The denominator represents the ohmic drop in the electrolyte over a field line.

The numerator is easily obtained as the inverse of the derivative of the polarization curve at the average cathodic current density, j_c . For the recommended current density of 200 A/m², this value is about 3.8^{E-4} V·m²/A at 100 RPM and about 3.2^{E-4} V·m²/A for higher RPM values.

The denominator requires a proper definition of the characteristic length L . For a first approximation, a suitable definition is the length between the most recessed and most protruding point of the part to be plated. When focusing on aviation landing gear parts, a typical value would be $L = 0.1$ m, which results in a Wagner number of about 0.04.

For Wagner numbers $\gg 1$, nearly no non-uniformity will occur (“secondary” current density distribution), while for $Wa \ll 1$, severe non-uniformity in current density and deposit thickness will occur (“primary” current density distribution).

Hence for Zn-Ni coatings being applied to large parts with important 3D topology on the surfaces to be plated, severe problems with the non-uniformity of current density, layer thickness and deposit composition can be expected. This suggests that dedicated conforming anode systems be used for each landing gear program, even beyond the state-of-art conforming anode systems as used for cadmium plating processes.

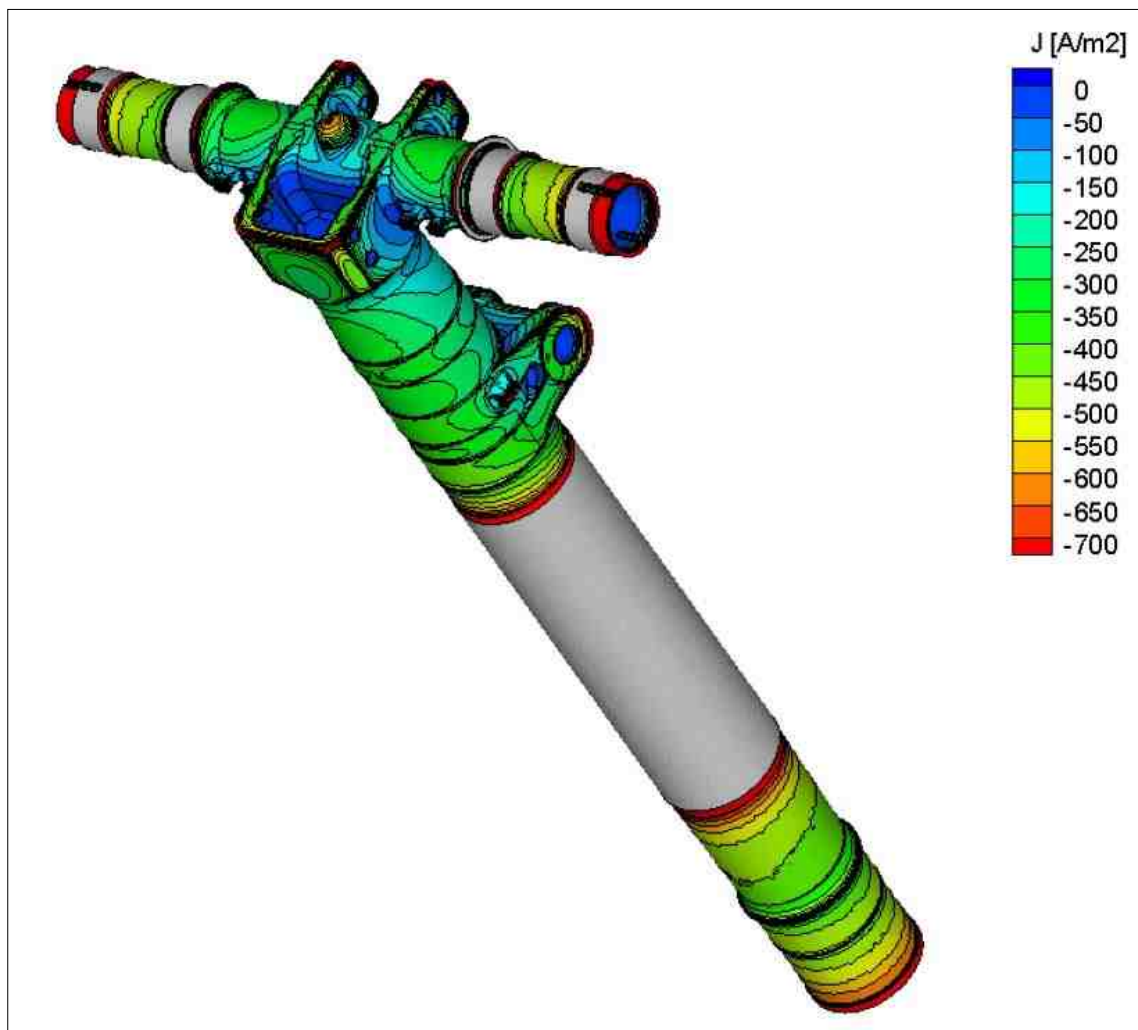


Figure 11—Simulated Zn-Ni current density distribution over a landing gear part.

In addition, the flow conditions (electrolyte refreshment) along the surfaces to be plated will be strongly dependent on the type and configuration of flow agitation used in the Zn-Ni plating tank, as well as on the geometry, positioning and orientation of the landing gear part in the tank. Given the fact that both total plating efficiency and alloy composition depend on the local flow conditions, a dedicated forced flow system for each landing gear part programs also seems unavoidable.

The polarization resistance can be influenced by changing the electrolyte composition, in particular the additives (type and concentration). Additives such as levelers and brighteners can lower the slope of the polarization curve, especially in the region below 200 A/m². However, this is only possible for kinetically-controlled plating processes. It will not affect a plating process that is under complete mass transfer control.

The conductivity of this Zn-Ni electrolyte is similar to the conductivity of some widely used electrolytes, such as Watts and sulfamate nickel baths. Nonetheless, it is worth noting that - for example - for industrial acid copper plating solutions, the conductivity is easily five times higher, and the additives being used commercially often lower the polarization resistance significantly. As a result, most industrial acid copper plating baths have a throwing power that by far outperform the throwing power of Zn/Ni baths.

Electrolyte maintenance

As for most alloy plating electrolytes, maintenance of the Zn/Ni electrolyte is critical. Different commercial electrolytes have different approaches to the configuration of the additives. Often suppliers group a set of additives in one solution while some supply the components individually. In the present case, a set of five different additives was necessary to maintain/correct the electrolyte to within the specified tolerances. In addition to organic additives, the nickel concentration is also maintained by dosing a nickel concentrate solution, while zinc is often replenished using metallic zinc. Unlike other electrolytes where metal pellets are used as anodes in the plating tank, in Zn/Ni electrolytes, the metallic zinc dissolves by chemical dissolution in a separate tank. To maintain the zinc concentration, a volume of this zinc-rich electrolyte is added to the main electrolyte on an ampere-hour (A-hr) basis.

To maintain the metal ratio in the electrolyte properly, monitoring is required at least twice a day, preferentially by x-ray fluorescence or alternatively by titration. If nickel is easy to replenish, care must be taken to ensure a constant zinc concentration in the zinc dissolution tank.

Despite each additive / metal being added continuously during production, this delicate balance is disrupted more often than

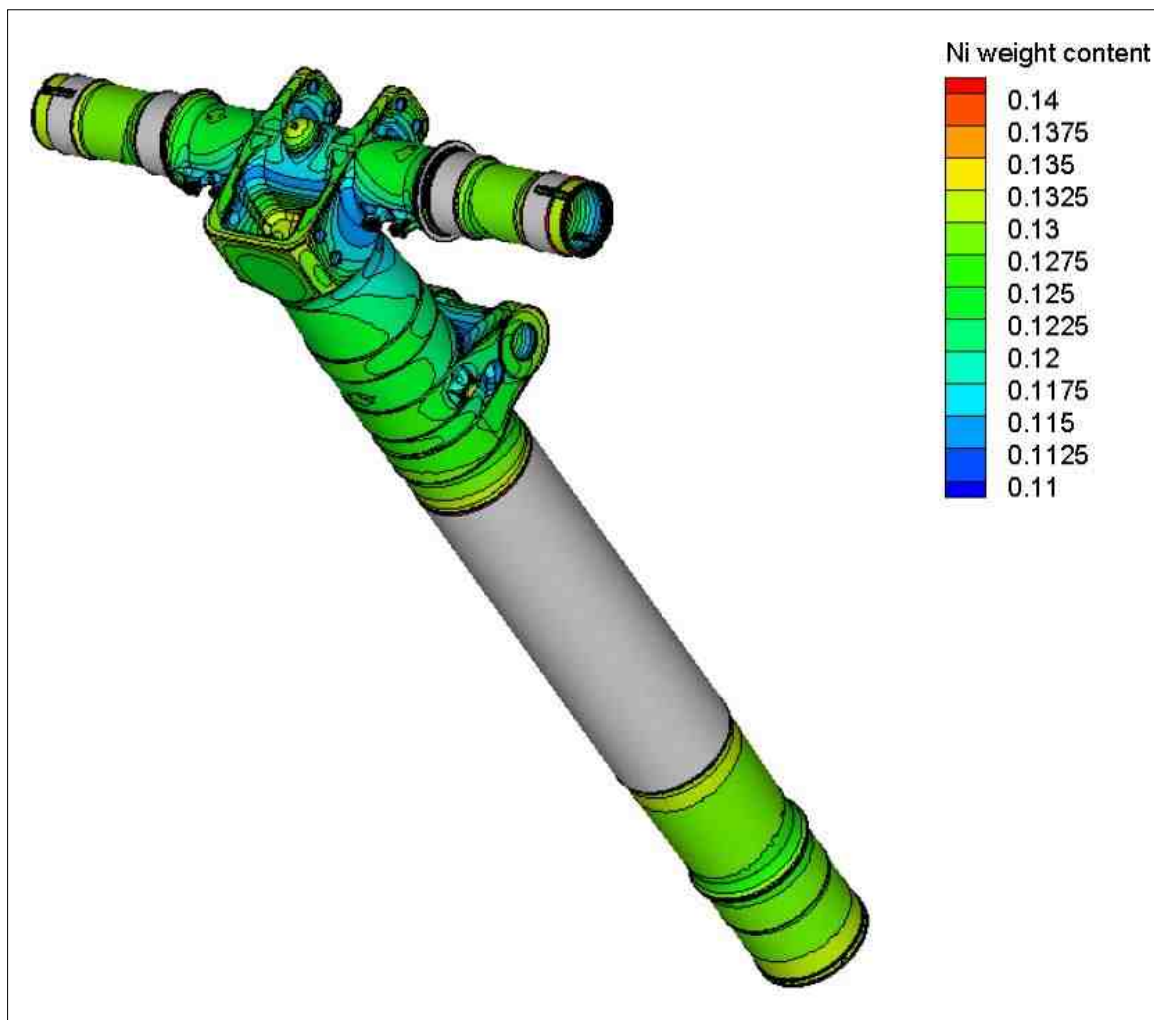


Figure 12—Simulated nickel content in the Zn-Ni deposit over a landing gear part.

desired and scrap rates consequently increase dramatically. Since most companies do not possess the advanced analytical techniques to quantify organic additives properly, only an empirical approach remains to ensure a balanced electrolyte. This often relies on a number of Hull cell panels made with different additive concentrations to determine the best corrective action.

Although Zn/Ni works very well when balanced, it is not an easy electrolyte to maintain either preventively or correctively.

Conclusions

It has been stated that 15 wt% nickel is the threshold above which corrosion resistance drops significantly. In the scope of the present study, it has been seen that for a broad range of current densities and flow conditions the deposit remains below this level.

However, it has also been stated that the electrolyte under study was used with a nickel concentration at the lower end of the recommended concentration window, which prevented exceeding the 15 wt% limit at higher current densities, but at the normal range of current density values. This type of electrolyte is designed to produce an alloy with at least 12 wt% nickel, below which corrosion protection is also reduced.

As seen in the previous section, electrolyte maintenance is not trivial and a lack of balance in metals or additives can easily promote a shift to higher nickel contents, thereby exceeding the 15 wt% limit.

Due to the low Wagner number values that are encountered for this electrolyte, the use of properly designed conforming anodes will be unavoidable for nearly any aerospace component being Zn/Ni plated.































The sensitivity of the nickel content in the deposit to flow conditions is also evidence for well-controlled flow conditions.

Similar performance studies could be made for other Zn/Ni baths (e.g., acidic ones) or even other candidate cadmium replacing alloy plating systems, such as Sn/Zn.

References

1. M. Nelson & E. Groshart, *Metal Finishing*, **95** (2), 79 (1997).
2. E.W. Brooman, *Metal Finishing*, **98** (4), 42 (2000).
3. C.M. Vlad, in *TMS Symposium on Zinc-based Steel Coating Systems*, G. Krauss and D.K. Matlock, Eds., The Minerals, Metals and Materials Society (TMS), Warrendale, PA, 2000; p. 129.
4. M. Pushpavanam, *et al.*, *J. Appl. Electrochem.*, **21** (7), 642 (1991).
5. A.M. Alfantasi, *A Study on the Synthesis, Characterization and Properties of Pulse-Plated Ultrafine-Grained Zn-Ni Alloy Coating*, Ph.D. thesis, Queen's University, Kingston, Ontario, 1994.
6. H. Park & J.A. Szpunar, *Corrosion Sci.*, **40** (4-5), 525 (1998).
7. M. Benballa, *et al.*, *Surf. Coat. Technol.*, **123** (1), 55 (2000).
8. M. Heydarzadeh Sohi & M. Jalali, *J. Mater. Process. Technol.*, **138** (1-3), 63 (2003).
9. Bruet-Hotellaz, *et al.*, *J. Mater. Sci.*, **34**, 881 (1999).
10. M.R. Lambert, R.G. Hart & H.E. Townsend, SAE Tech. Paper #831817, SAE International, Warrendale, PA, 1983.
11. G.D. Wilcox & D.R. Gabe, *Corrosion Sci.*, **35** (5-8), 1251 (1993).
12. M. Gavrilu, *et al.*, *Surf. Coat. Technol.*, **123** (2-3), 164 (2000).

Addendum - RDE Text Matrix Results

		Rotating Disc Speed (RPM)		
		100	400	1200
Current Density, A/m ²	22			
	50			
	100			
	150			
	200			
	250			
	300			
	400			
	800			
	1600			

About the authors



Paulo Vieira graduated from the Universidade de Coimbra (Portugal) with a licentiate degree in Industrial Chemistry in 2005. Paulo then joined Electrofer IV, a leading automotive electroplating company in Portugal where he first held responsibilities in production. Paulo became responsible for Process Development in 2007, ensuring process optimization, testing and approval of prototype parts. In 2008, Paulo joined Elsyca's engineering team where he currently works on consulting projects as a project engineer. Paulo has been active mainly in functional plating but also in decorative plating, electropolishing and electrocoating.



Dr. Bart Van den Bossche graduated from the Vrije Universiteit Brussel (VUB, Belgium) with a M.Sc. degree in Metallurgical Engineering in 1991. He received a Ph.D. in Electrochemical Engineering in 1998. Bart is Elsyca's Engineering Manager for Surface Finishing projects. Bart has been active in electrochemical process computer modeling for over 15 years, as reflected in a series of peer reviewed papers. In addition, Bart has a long track record as a consultant for electrochemical cell and tooling design in the plating, electroforming and electrochemical machining industry. As Elsyca co-founder, Bart is in charge of several Elsyca consulting projects.



Dr. Alan Rose is an elected fellow of the Institute of Mechanical Engineers in the U.K., with a B.Sc. in Aeronautical Engineering and a Ph.D. in Chemical and Process Engineering. He currently holds Research Fellow positions at Manchester University and Liverpool University, where he has been involved in flow-related research and training of graduates and post-graduates in computational fluid dynamics. Dr. Rose is a long-time advocate of engineering simulation tools and has been involved in verification, validation, implementation and simulation programs with the U.S. Air Force, Rolls-Royce, DuPont and Johnson Matthey, to mention a few. For the past five years, he has been instrumental in the adoption and application of software simulation tools in electrochemical process industries, such as plating, machining and even corrosion. Dr. Rose is currently based in Atlanta and is responsible for Elsyca's North American business.



AESF Foundation Research Program

The AESF Research Program began in 1919 when Dr. William Blum asked the Society to help fund research efforts of the National Bureau of Standards (now the National Institute of Science and Technology). This initial request paved the way for the expansion of the AESF Research Program in 1944 to support universities and colleges, industrial companies, and independent research centers and laboratories. This program will continue to expand and thrive under the direction of the AESF Foundation.

In the past, the AESF Research Program has awarded grants for the following projects:

- University of South Carolina, "Development of New Process for Plating Thin Films of Zn-Ni-P-X, etc."
- Pennsylvania State University, "Development of Environmentally Friendly Corrosion Prevention Deposit on Steel"
- University of Cincinnati, "Improved Silane Film Performance by Electrodeposition"
- McGill University, "Effect of Material Characteristics and Surface Processing Variables on Hydrogen Embrittlement of Steel Fasteners" (part of a 3-year research project)
- University of South Carolina, "Development of Ni Based High Wear Resistance Composite Coatings"



The AESF Foundation's goals are to encourage and support activities that help progress the science and technology of the surface finishing industry. Pertinent R&D activities, conducted or sponsored by the industry, universities and government agencies can provide new resources and the Foundation is seeking projects to fund that will help to achieve its goals.

To contribute to the AESF Foundation and the Research Program [CLICK HERE](#).